

# Turbulence compensation of an orbital angular momentum and polarization-multiplexed link using a data-carrying beacon on a separate wavelength

Yongxiong Ren,<sup>1,\*</sup> Guodong Xie,<sup>1</sup> Hao Huang,<sup>1</sup> Long Li,<sup>1</sup> Nisar Ahmed,<sup>1</sup> Yan Yan,<sup>1</sup> Martin P. J. Lavery,<sup>2</sup> Robert Bock,<sup>3</sup> Moshe Tur,<sup>4</sup> Mark A. Neifeld,<sup>5</sup> Robert W. Boyd,<sup>2,6</sup> Jeffrey H. Shapiro,<sup>7</sup> and Alan E. Willner<sup>1</sup>

<sup>1</sup>Department of Electrical Engineering, University of Southern California, Los Angeles, California 90089, USA

<sup>2</sup>School of Physics and Astronomy, University of Glasgow, Glasgow G12 8QQ, UK

<sup>3</sup>R-DEX Systems, Marietta, Georgia 30068, USA

<sup>4</sup>School of Electrical Engineering, Tel Aviv University, Tel Aviv 69978, Israel

<sup>5</sup>Department of Electrical and Computer Engineering, University of Arizona, Tucson, Arizona 85721, USA

<sup>6</sup>Department of Physics and Astronomy, The Institute of Optics, University of Rochester, Rochester, New York 14627, USA

<sup>7</sup>Massachusetts Institute of Technology, Research Laboratory of Electronics, Cambridge, Massachusetts 02139, USA

\*Corresponding author: yongxior@usc.edu

Received February 27, 2015; revised April 3, 2015; accepted April 11, 2015;  
posted April 13, 2015 (Doc. ID 233828); published May 6, 2015

We investigate the sensing of a data-carrying Gaussian beacon on a separate wavelength as a means to provide the information necessary to compensate for the effects of atmospheric turbulence on orbital angular momentum (OAM) and polarization-multiplexed beams in a free-space optical link. The influence of the Gaussian beacon's wavelength on the compensation of the OAM beams at 1560 nm is experimentally studied. It is found that the compensation performance degrades slowly with the increase in the beacon's wavelength offset, in the 1520–1590 nm band, from the OAM beams. Using this scheme, we experimentally demonstrate a 1 Tbit/s OAM and polarization-multiplexed link through emulated dynamic turbulence with a data-carrying beacon at 1550 nm. The experimental results show that the turbulence effects on all 10 data channels, each carrying a 100 Gbit/s signal, are mitigated efficiently, and the power penalties after compensation are below 5.9 dB for all channels. The results of our work might be helpful for the future implementation of a high-capacity OAM, polarization and wavelength-multiplexed free-space optical link that is affected by atmospheric turbulence. © 2015 Optical Society of America

OCIS codes: (010.1080) Active or adaptive optics; (010.1330) Atmospheric turbulence; (060.2605) Free-space optical communication; (060.4230) Multiplexing.  
<http://dx.doi.org/10.1364/OL.40.002249>

Free-space optical communications that use multiplexed orthogonal spatial modes have the potential to greatly increase system capacity and spectral efficiency by transmitting multiple data-carrying beams in the same spectral band [1–4]. A modal set that has gained interest in this regard is the orbital angular momentum (OAM) basis.

A light beam that has a helical wavefront carries an OAM corresponding to  $\ell\hbar$  per photon, where  $\hbar$  is the reduced Planck constant and  $\ell$  is an unbounded integer [5]. OAM beams with different  $\ell$  values are mutually orthogonal, so that beams carrying different OAMs can act as independent data channels for efficiently multiplexing multiple information-bearing signals in a communication system [3,4,6]. Importantly, OAM multiplexing is, in principle, compatible with the existing wavelength and polarization-multiplexing techniques.

Previous work has demonstrated Terabit/s free-space data transmissions using OAM multiplexing in a laboratory setting with no atmospheric turbulence effects [3]. It is well known that turbulence distorts OAM beams, which may decrease the power received after demultiplexing from the desired channel and introduce intermodal crosstalk between channels [7–13]. Multiple-input and multiple-output (MIMO) digital signal processing (DSP), which is widely used in radio-frequency links and fiber-based mode division multiplexing systems [14], has been implemented to mitigate the crosstalk between

OAM channels [15]. Optical compensation of turbulence-induced phase-front distortions of OAM beams can also reduce these effects, providing a complementary approach to MIMO DSP [16–18]. Recently, it has been experimentally demonstrated that adaptive optics (AO)-based turbulence compensation of multiple OAM beams can be realized using a specially designed AO system at the receiver [19–21]. By exploiting the fact that turbulence creates negligible depolarization [22], a polarized Gaussian beam was used to probe the turbulence and obtain the correction patterns for compensating the OAM beams on the orthogonal polarization. This approach, however, sacrifices the polarization degree of freedom for multiplexing.

In this Letter, we propose the use of a data-carrying Gaussian beacon on a separate wavelength as a means to provide the information needed to compensate for the effects of turbulence in an OAM and polarization-multiplexed link [23]. The influence of the wavelength difference between the Gaussian beacon and the 1560 nm OAM beams is investigated. We find that the compensation performance degrades slowly as the wavelength difference increases in the 1520–1590 nm band. With this scheme, we experimentally demonstrate a 1 Tbit/s OAM and polarization-multiplexed link through emulated dynamic turbulence with a temporal bandwidth of ~2 Hz. Eight OAM beams at 1560 nm and two 1550 nm Gaussian

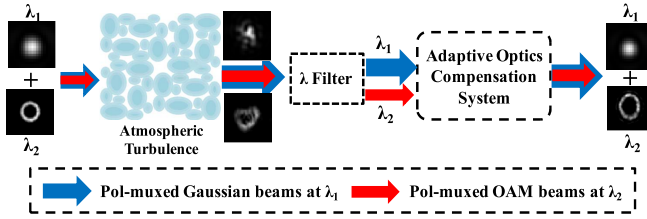


Fig. 1. Concept diagram. The pol-muxed Gaussian beam at  $\lambda_1$  is separated from the pol-muxed OAM beams at  $\lambda_2$  by using a free-space bandpass filter. It then acts as a beacon for wavefront sensing and correction.

beams ( $\ell = 0$ ) with polarization multiplexing are transmitted. Each beam carries a 100 Gbit/s signal, thus allowing a total capacity of 1 Tbit/s. The experimental results show that the power penalties with the proposed scheme are below 5.9 dB for all ten channels.

The concept for our compensation scheme is shown in Fig. 1. Polarization-multiplexed (pol-muxed) Gaussian beams at  $\lambda_1$  propagate coaxially with multiple pol-muxed OAM beams at  $\lambda_2$  through atmospheric turbulence. At the receiver, a Gaussian beam on one of the polarizations at  $\lambda_1$  is filtered out and sent to an AO compensation system. This Gaussian beam serves as a probe for wavefront sensing, from which the required correction patterns are retrieved. The correction patterns obtained are used to compensate all the distorted OAM and Gaussian beams.

The experimental setup is presented in Fig. 2. A quadrature phase-shift keying (QPSK) transmitter produces 100 Gbit/s signals at wavelengths  $\lambda_1$  and  $\lambda_2$ , where  $\lambda_1$  is tunable and  $\lambda_2$  is fixed at 1560 nm. The  $\lambda_2$ -wavelength QPSK signal is split into four copies, each of which is delayed using a different length of single-mode fiber (SMF) to de-correlate the data sequences. These four signal beams are collimated in free space and converted into four different OAM beams by two spatial light modulators (SLMs 1 and 2). Specifically, the surface of each SLM is divided into two equal-sized regions, each of which is loaded with the specific spiral-phase hologram needed to convert one of the incoming Gaussian beams into the desired OAM beam (OAM  $\ell = \pm 2$  or  $\pm 5$ ). The four OAM beams at  $\lambda_2 = 1560$  nm are then spatially multiplexed using three beam splitters (BSs 1, 2, and 3).

The  $\lambda_1$ -wavelength beam, which also carries a QPSK channel, is converted into a collimated Gaussian beam ( $\ell = 0$ ) to act as the beacon for compensation. This beacon beam is then expanded using a  $4f$  lens system to become as wide as the widest OAM beam. Next, the expanded beacon is combined with the OAM beams (BS-4) and polarization multiplexed by a pair of polarizing beam splitters, which are arranged to introduce a 270 ps delay between the orthogonal polarizations. The resulting pol-muxed OAM and Gaussian beacon beams then propagate coaxially to our turbulence emulator.

Atmospheric turbulence is emulated here by a thin rotating phase screen whose pseudo-random phase distribution obeys Kolmogorov spectrum statistics [11]. It is characterized by the effective Fried coherence length  $r_0$ , given by [24,25]

$$r_0 = \left( 0.423 \left( \frac{2\pi}{\lambda} \right)^2 C_n^2 d \right)^{-0.5},$$

where  $\lambda$  is the optical wavelength,  $C_n^2$  is the atmospheric structure constant, and  $d$  is the thickness of the phase screen. In our experiment,  $r_0$  is set to be 1 mm at 1550 nm, which could represent weak-to-moderate turbulence over a 1 km link distance [11,24]. Because  $r_0$  is proportional to  $\lambda^{6/5}$ , and changes slightly around 1550 nm, two beams with wavelengths close to 1550 nm may experience similar turbulence distortions. We note that for a longer link distance, diffraction effects should be considered. Our turbulence emulator is a thin screen, hence it may not adequately represent uniformly distributed (thick) turbulence [24,25].

At the receiver, the proposed AO compensation scheme is implemented in a closed-loop configuration. The beams at the exit plane of the turbulence emulator are imaged onto the wavefront corrector (SLM-3) inside the AO system by using a  $4f$  lens system. As SLM-3 is polarization sensitive, a half-wave plate is used to align one of the incoming beams' polarization with SLM-3's polarization orientation. We note that a pair of polarization-sensitive wavefront correctors would be required to correct the pol-muxed beams simultaneously. In order to use the Gaussian beam at  $\lambda_1$  as a beacon for wavefront

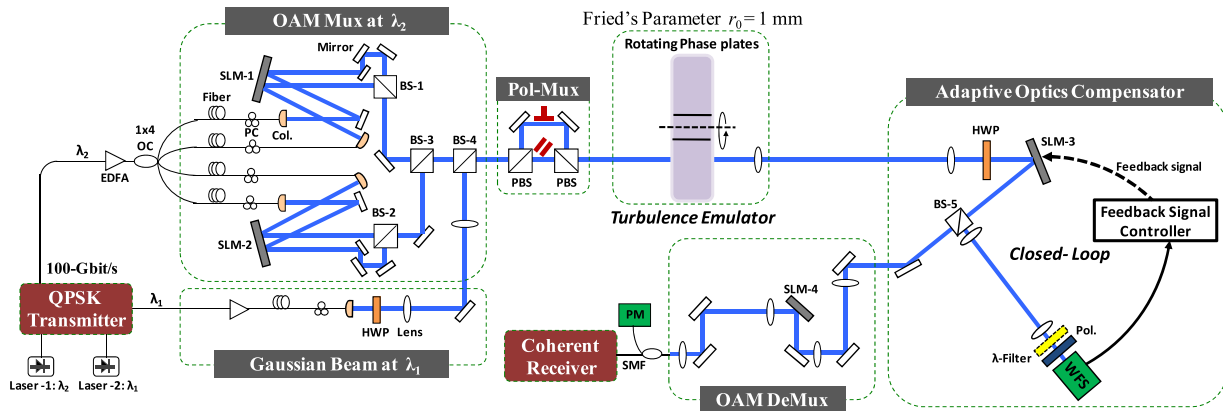


Fig. 2. Experimental setup. BS: beam splitter; Col.: Collimator; EDFA: erbium-doped fiber amplifier; OAM: orbital angular momentum; OC: optical coupler; DeMux: demultiplexing; Mux: multiplexing; PBS: polarizing beam splitter; PC: polarization controller; PM: power meter; Pol.: Polarizer; Pol-Mux: polarization multiplexing; QPSK: quadrature phase-shift keying; WFS: Shack-Hartmann wavefront sensor.

sensing, a small portion of the beam reflected by SLM-3 is directed by a beam splitter (BS-5) toward a combination of a free-space, narrow band-pass optical filter centered on  $\lambda_1$  and a polarizer to filter out all OAM modes with  $\ell \neq 0$ . The wavefront of the polarized Gaussian beacon emerging SLM-3 is then imaged onto a Shack-Hartmann wavefront sensor (WFS) to detect the beacon's residual wavefront distortions. Up to the 19th-order Zernike polynomial is used in the WFS for wavefront estimations. A feedback controller then dynamically feeds SLM-3 with the appropriate turbulence-dependent correction patterns. The patterns obtained from the Gaussian beacon at  $\lambda_1$  are directly utilized for the simultaneous compensation of all distorted beams, including the OAM beams at  $\lambda_2$ . We note that the proper phase conversion between  $\lambda_1$  and  $\lambda_2$  can also be performed to achieve a more accurate compensation for the  $\lambda_2$  beams.

After wavefront correction, the multiplexed beams are then sent to SLM-4, which is loaded with the inverse spiral-phase hologram that converts the OAM beam of a particular channel chosen for detection back into a Gaussian-like beam. Note that SLM-4 is loaded with a blank pattern—so it acts like a simple mirror—when demultiplexing either of the Gaussian channels. The beam after SLM-4 is then coupled into an SMF and sent for coherent detection and offline DSP.

Figure 3 depicts the received powers of OAM channels  $\ell = +2$  and  $+5$  after wavefront compensation and demultiplexing for various Gaussian beacon wavelengths  $\lambda_1$  under a random turbulence realization. Here, only one channel (either  $\ell = +2$  or  $\ell = +5$ ) in the  $\lambda_2$  branch is on. We see that the received power curves for both channels are relatively flat. The highest received power for OAM  $\ell = +2$  is obtained when  $\lambda_1 = \lambda_2$ . Figure 4 shows the bit error rate (BER) when only channel  $\ell = +2$  [see Fig. 4(a)] or  $\ell = +5$  [see Fig. 4(b)] is transmitted with beacon wavelengths  $\lambda_1 = 1520$ ,  $1560$ , and  $1590$  nm, over 10 random turbulence realizations. We see that lowest BER is reached at  $\lambda_1 = \lambda_2$ , as expected.

We then turn on all the  $\lambda_2$  channels and set  $\lambda_1 = 1560$  nm to investigate the average BER performance in a dynamic turbulence condition that is emulated by rotating the phase screen plate. Each data channel experiences time-varying signal fading and crosstalk as the phase plate rotates. Figure 5 shows the recovered QPSK constellations of the  $X$ -polarized OAM channels  $\ell = +2$  and  $\ell = +5$  for two random turbulence realizations.

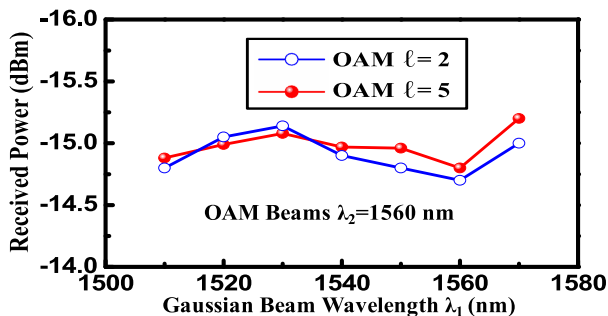


Fig. 3. SMF-coupled power after wavefront compensation and demultiplexing for OAM channels  $\ell = +2$  and  $+5$  as a function of the Gaussian beacon's wavelength.

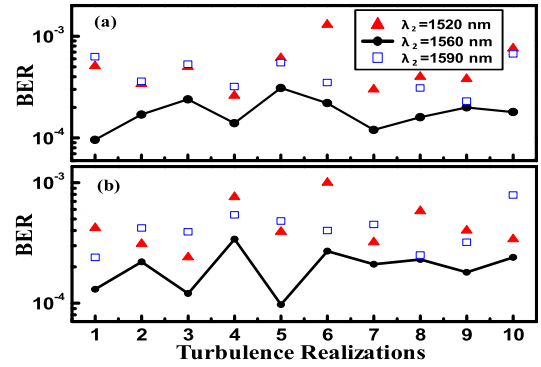


Fig. 4. Measured BER of OAM channels  $\ell = +2$  and  $\ell = +5$  for various Gaussian beacon wavelengths.

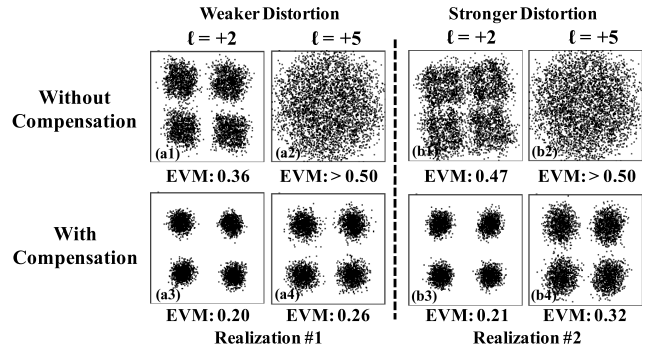


Fig. 5. Recovered constellations of the  $X$ -polarized channels  $\ell = +2$  (a1–a4) and  $+5$  (b1–b4) with and without compensation. EVM: error vector magnitude.

The error vector magnitude value of each constellation is also shown. We see that the constellations of both channels become better defined after compensation. The constellations of channel  $\ell = +2$  exhibit better quality than those of channel  $\ell = +5$  because OAM beam  $\ell = +5$  is larger than OAM beam  $\ell = +2$ ; thus, it suffers more phase distortions.

Owing to the frequency limits imposed by the wavefront corrector and the WFS, our AO system's maximum working bandwidth is  $\sim 2$  Hz. Consequently, we control the rotation rate of the phase screen to emulate dynamic turbulence with a 2 Hz temporal bandwidth [11]. We note that typically, the temporal bandwidth (cutoff frequency) of atmospheric turbulence is about 0.1–1 kHz [26]. Figure 6 shows the average BER as a function of optical signal-to-noise ratio (OSNR) for OAM channels  $\ell = +2$  and  $\ell = +5$  on both  $X$ - and  $Y$ -polarizations. The BERs for each channel are extremely high without compensation ( $> 5 \times 10^{-2}$ ) because of the severe crosstalk and are not shown. However, all of the BER curves after compensation are below the forward error correction (FEC) threshold of  $1 \times 10^{-3}$  when OSNR is greater than 16.5 dB. Figure 7 shows the measured power penalties at the  $1 \times 10^{-3}$  FEC threshold for all of the Gaussian and OAM channels. We see that after compensation, the power penalties of all channels, as compared to their respective back-to-back counterparts, are below 5.9 dB. We also observe that the  $X$ -polarized channels have lower power penalties than the  $Y$ -polarized channels. This is possibly because the wavefront correct, which

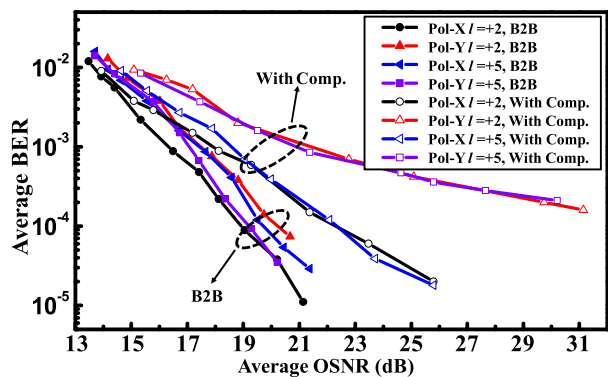


Fig. 6. Average BERs for OAM channels  $\ell = +2$  and  $+5$  on both  $X$ - and  $Y$ -polarizations (Pol- $X$  and Pol- $Y$ ). B2B (back-to-back) is the no-turbulence case. The BERs for all channels without compensation (not shown) exceed  $5 \times 10^{-2}$ .

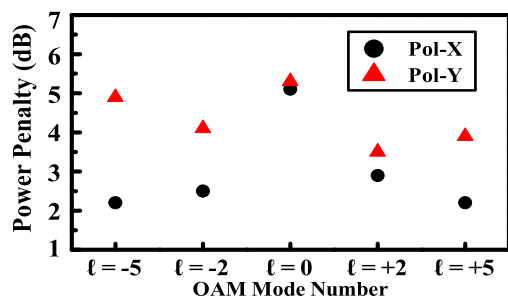


Fig. 7. Measured power penalties for all Gaussian ( $\ell = 0$ ) and OAM channels ( $\ell = \pm 2$  and  $\pm 5$ ).

is a polarization-sensitive SLM in our experiment, performs more efficient phase modulation for  $X$ -polarized beams.

In conclusion, we have proposed and demonstrated the use of a data-carrying Gaussian beacon on a separate wavelength for turbulence compensation of an OAM and polarization-multiplexed free-space optical link. The influence of the wavelength offset between the Gaussian beacon and the OAM beams on the compensation performance of all multiplexed beams was investigated. Using this scheme, we experimentally demonstrated a 1 Tbit/s OAM and polarization-multiplexed link through emulated dynamic turbulence, with post-compensation power penalties below 5.9 dB for all channels. This approach could also be potentially applied to OAM-based quantum communications [26].

We thank Jerome Ballesta, Baris Erkmen, and Michael Kendra for fruitful discussions. We acknowledge the generous support of the Air Force Office of Scientific Research.

## References

1. G. Gibson, J. Courtial, M. Padgett, M. Vasnetsov, V. Pas'ko, S. Barnett, and S. Franke-Arnold, *Opt. Express* **12**, 5448 (2004).

2. I. B. Djordjevic and M. Arabaci, *Opt. Express* **18**, 24722 (2010).
3. J. Wang, J.-Y. Yang, I. M. Fazal, N. Ahmed, Y. Yan, H. Huang, Y. Ren, Y. Yue, S. Dolinar, M. Tur, and A. E. Willner, *Nat. Photonics* **6**, 488 (2012).
4. T. Su, R. P. Scott, S. S. Djordjevic, N. K. Fontaine, D. J. Geisler, X. Cai, and S. J. B. Yoo, *Opt. Express* **20**, 9396 (2012).
5. L. Allen, M. W. Beijersbergen, R. J. C. Spreeuw, and J. P. Woerdman, *Phys. Rev. A* **45**, 8185 (1992).
6. N. Bozinovic, Y. Yue, Y. Ren, M. Tur, P. Kristensen, H. Huang, A. E. Willner, and S. Ramachandran, *Science* **340**, 1545 (2013).
7. C. Paterson, *Phys. Rev. Lett.* **94**, 153901 (2005).
8. J. A. Anguita, M. A. Neifeld, and B. V. Vasic, *Appl. Opt.* **47**, 2414 (2008).
9. G. A. Tyler and R. W. Boyd, *Opt. Lett.* **34**, 142 (2009).
10. B. Rodenburg, M. P. J. Lavery, M. Malik, M. N. O'sullivan, M. Mirhosseini, D. J. Robertson, M. Padgett, and R. W. Boyd, *Opt. Lett.* **37**, 3735 (2012).
11. Y. Ren, H. Huang, G. Xie, N. Ahmed, Y. Yan, B. I. Erkmen, N. Chandrasekaran, M. P. J. Lavery, N. K. Steinhoff, M. Tur, S. Dolinar, M. Neifeld, M. J. Padgett, R. W. Boyd, J. H. Shapiro, and A. E. Willner, *Opt. Lett.* **38**, 4062 (2013).
12. N. Chandrasekaran and J. H. Shapiro, *J. Lightwave Technol.* **32**, 1075 (2014).
13. M. Krenn, R. Fickler, M. Fink, J. Handsteiner, M. Malik, T. Scheidl, R. Ursin, and A. Zeilinger, *New J. Phys.* **16**, 113028 (2014).
14. P. J. Winzer and G. J. Foschini, *Opt. Express* **19**, 16680 (2011).
15. H. Huang, Y. Cao, G. Xie, Y. Ren, Y. Yan, C. Bao, N. Ahmed, M. A. Neifeld, S. J. Dolinar, and A. E. Willner, *Opt. Lett.* **39**, 4360 (2014).
16. B. L. Ellerbroek, *J. Opt. Soc. Am. A* **11**, 783 (1994).
17. G. D. Love, *Appl. Opt.* **36**, 1517 (1997).
18. K. Murphy, D. Burke, N. Devaney, and C. Dainty, *Opt. Express* **18**, 15448 (2010).
19. Y. Ren, G. Xie, H. Huang, C. Bao, Y. Yan, N. Ahmed, M. P. J. Lavery, B. I. Erkmen, S. Dolinar, M. Tur, M. A. Neifeld, M. J. Padgett, R. W. Boyd, J. H. Shapiro, and A. E. Willner, *Opt. Lett.* **39**, 2845 (2014).
20. B. Rodenburg, M. Mirhosseini, M. Malik, O. S. Magaña-Loaiza, M. Yanakas, L. Maher, N. Steinhoff, G. Tyler, and R. W. Boyd, *New J. Phys.* **16**, 033020 (2014).
21. Y. Ren, G. Xie, H. Huang, N. Ahmed, Y. Yan, L. Li, C. Bao, M. P. J. Lavery, M. Tur, M. Neifeld, R. W. Boyd, J. H. Shapiro, and A. E. Willner, *Optica* **1**, 376 (2014).
22. M. Toyoshima, H. Takenaka, Y. Shoji, Y. Takayama, Y. Koyama, and H. Kunimori, *Opt. Express* **17**, 22333 (2009).
23. Y. Ren, G. Xie, H. Huang, L. Li, N. Ahmed, Y. Yan, M. Lavery, M. Tur, M. Neifeld, S. Dolinar, M. Padgett, R. W. Boyd, J. H. Shapiro, and A. E. Willner, "1-Tbit/s orbital angular-momentum multiplexed FSO link through emulated turbulence with a data-carrying beacon on a separate wavelength for compensation," in *Frontiers in Optics (FiO) 2014*, Tucson, Arizona, 2014, paper FTH3B.7.
24. L. Andrews, R. Phillips, and A. R. Weeks, *Waves Random Media* **7**, 229 (1997).
25. D. L. Fried and H. T. Yura, *J. Opt. Soc. Am.* **62**, 600 (1972).
26. M. Mirhosseini, O. Magaña-Loaiza, M. N. O'Sullivan, B. Rodenburg, M. Malik, M. P. J. Lavery, M. J. Padgett, D. J. Gauthier, and R. W. Boyd, *New J. Phys.* **17**, 033033 (2015).